



*Supplement of*

## **A human-portable mass flux method for methane emissions quantification: controlled release testing performance evaluation**

**Coleman Vollrath et al.**

*Correspondence to:* Coleman Vollrath (coleman.vollrath1@ucalgary.ca)

The copyright of individual parts of the supplement might differ from the article licence.

**S1. Description of pneumatic “trough” or “trap” method to determine the CH<sub>4</sub> content of the gas released from each CNG tank during the experiments.**

A pneumatic trough, or water trap, is a simple and effective method for collecting small gas samples that do not readily dissolve in water. Water is used to isolate the sample from atmospheric contaminants. To begin, a sample syringe was submerged upright in a bucket filled with water, displacing any existing gas inside. Once the syringe was void of atmospheric gas, it was inverted, and gas was introduced into the bucket at the bottom of the syringe using a hose. As gas flowed in, it displaced the water in the syringe. When the syringe was sufficiently filled with gas, we inserted a plunger into the syringe while keeping it inverted and underwater, sealing the gas inside. The syringe was then removed from the water, and a needle was attached to transfer the gas into a vacated septa bottle for storage and analysis. Multiple samples were collected for redundancy. Samples were analyzed using gas chromatography. Any sample contaminated with atmospheric gases such as O<sub>2</sub> or CO<sub>2</sub> were excluded from analysis. The CH<sub>4</sub> content of the remaining samples was averaged to determine the CH<sub>4</sub> content of the gas released during the experiments. We used this to correct the bulk gas release rates.

**Table S1. Release rates, experiment times, and downwind measurement distances.**

Date	Start time	End time	Release rate (kg CH <sub>4</sub> /h)	Downwind distance (m)
12-Jun-24	12:28:40	12:40:19	0.20	15
12-Jun-24	12:45:10	12:58:55	0.20	30
06-Aug-24	14:56:05	15:02:25	0.31	10
06-Aug-24	14:45:25	14:54:16	0.31	20
12-Jun-24	11:38:08	11:54:23	0.41	15
12-Jun-24	11:56:56	12:10:42	0.41	30
11-Jun-24	14:01:23	14:15:36	0.64	10
11-Jun-24	14:18:42	14:33:45	0.64	20
06-Aug-24	14:10:21	14:17:52	0.82	15
06-Aug-24	13:58:01	14:08:28	0.82	30
11-Jun-24	16:58:33	17:05:48	0.92	10
11-Jun-24	17:07:54	17:16:35	0.92	20
12-Jun-24	13:41:56	13:50:25	1.15	15
12-Jun-24	13:53:03	14:04:20	1.15	30
11-Jun-24	14:46:07	14:54:59	1.28	10
11-Jun-24	14:58:04	15:09:48	1.28	20
06-Aug-24	16:04:38	16:11:22	1.53	10
06-Aug-24	15:53:30	16:02:26	1.53	20

12-Jun-24	14:11:47	14:19:14	1.79	15
06-Aug-24	12:22:19	12:30:47	1.79	15
06-Aug-24	12:08:06	12:20:24	1.79	30
12-Jun-24	14:21:12	14:31:07	1.79	30
11-Jun-24	15:22:25	15:29	1.99	10
11-Jun-24	15:32:02	15:40:46	1.99	20
06-Aug-24	12:46:54	12:56:36	2.30	15
06-Aug-24	12:34:11	12:45:20	2.30	30
12-Jun-24	14:40:40	14:48:14	2.40	15
12-Jun-24	14:50:03	14:59:13	2.40	30
06-Aug-24	15:08:58	15:17:49	2.63	20
11-Jun-24	15:50:39	15:57:59	2.63	10
06-Aug-24	15:19:31	15:26:03	2.63	10
11-Jun-24	16:01:59	16:12:15	2.63	20
11-Jun-24	16:35:53	16:43:26	3.27	10
06-Aug-24	15:41:10	15:47:41	3.27	10
11-Jun-24	16:45:04	16:55:01	3.27	20
06-Aug-24	15:29:53	15:39:24	3.27	20
06-Aug-24	13:13:42	13:22:06	3.83	15
06-Aug-24	13:00:55	13:11:40	3.83	30
12-Jun-24	15:07:47	15:15:38	3.94	15
12-Jun-24	15:17:29	15:27:25	3.94	30
12-Jun-24	15:35:15	15:42:08	4.86	15
12-Jun-24	15:44:00	15:55:27	4.86	30
12-Jun-24	16:01:44	16:09:06	5.62	15
12-Jun-24	16:10:20	16:21:06	5.62	30

## 15 S2. Flux plane sensitivity analysis.

Previous research studies that collected CH<sub>4</sub> mixing ratio data in the flux plane pattern (Rella et al., 2015) or used the method to quantify emissions rates (Nathan et al., 2015) indicated that the coefficient  $\alpha$  used in estimating the vertical wind profile and the size of the flux plane's grid cells could have small effects on the rate (4% to 10%). Thus, we performed a sensitivity analysis to assess changes in estimated CH<sub>4</sub> emissions rates as these variables changed.

20

We followed the same steps outlined in the methodology of the main text (Sect. 2.6.3) to quantify the release rates but changed the coefficient  $\alpha$  for estimating the vertical wind profile (Sect. 2.6.2) from 0.17 to 0.14 and 0.20. Release rates totalled 95.2 kg CH<sub>4</sub>/h. Using  $\alpha = 0.17$  to extrapolate wind propagated to 85.7 kg/h of quantified emissions as shown in the results in the main text. The values  $\alpha = 0.14$  and  $\alpha = 0.20$  resulted in a total of 85.9 kg/h and 85.6 kg/h of CH<sub>4</sub> emissions quantified, respectively, suggesting that our results are not sensitive to small changes to  $\alpha$ .

25

We set the size of the flux plane's grid cells to be 0.5 m<sup>2</sup>. Changing this to 0.35 m<sup>2</sup> and 1 m<sup>2</sup> similarly did not show substantial effects on the quantified rates. The total amount of emissions quantified with 0.5 m<sup>2</sup> grid cell resolution was 85.7 kg CH<sub>4</sub>/h compared to 95.2 kg/h of total released CH<sub>4</sub>. The total amount of emissions quantified with the 0.35 m<sup>2</sup> and 1 m<sup>2</sup> grid cell resolutions in the flux plane were 88.2 kg/h and 85.9 kg/h, respectively, indicating a 2.9% change to the quantified emissions at maximum.

30

### **S3. Justification for using Inverse Distance Weighted (IDW) squared for interpolating CH<sub>4</sub> mixing ratios.**

35

We chose IDW squared as our interpolation method because the influence of a measured point on an interpolated point decreases with distance, similar to how CH<sub>4</sub> mixing ratios in a plume decrease outward from the plume centerline as horizontal and vertical distances increase. Moreover, IDW is a deterministic interpolation method in that interpolated values are constrained within the range of minimum and maximum CH<sub>4</sub> mixing ratios measured. Using the inverse of the squared distance to determine the weight for each measured point in the interpolation was more accurate in estimating background CH<sub>4</sub> mixing ratios for grid cells directly outside of the plume compared to the inverse of the distance, which interpolated ~3 ppm for background CH<sub>4</sub>.

### **S4. Additional details on the vertical wind speed profile estimation.**

40

Rella et al. (2015) empirically determined  $\alpha = 0.17$  in controlled release testing experiments for the flux plane method using two anemometers to measure wind speed at different heights. This value was derived under slightly unstable atmospheric conditions, but moderate wind speeds of 6 m/s ± 1 m/s. Wind speeds measured during our experiments were similar or slightly lower. Rella et al.'s (2015) controlled release experiments were performed on flat terrain with short grasses, which is similar to the characteristics of the location where we performed our experiments. Thus, in the absence of empirical data to estimate  $\alpha$ , we adopted  $\alpha$  from Rella et al. (2015) to extrapolate wind speed measured during our experiments. Heier et al. (2014) reported a range of coefficients (0.14 to 0.17) based on measurements of wind speeds at 10 m and 30 m—presumably in a similar setting—to use for  $\alpha$  when wind speeds are ~4 m/s or greater. This reinforces that our use of Rella et al.'s (2015) wind shear coefficient was reasonable in extrapolating a vertical wind profile in the absence of an *in situ* estimate for  $\alpha$ . We tested other values for  $\alpha$  and found that our CH<sub>4</sub> rate estimates were not sensitive to slight changes to  $\alpha$  (see S2 for a sensitivity analysis).

50 **S5. CH<sub>4</sub> mixing ratios by measurement height for the experiment flagged by the second quality control criterion.**

The release in this experiment was 0.41 kg CH<sub>4</sub>/h performed at 30m downwind on 12 June 2024. The second quality control criterion flagged this experiment for not having decreasing CH<sub>4</sub> enhancements with height (see Fig S1 below), such that the enhancements at the top measurement level are one-half of the peak enhancement or less. Interpreting if we captured a sufficient amount of the plume in this experiment is challenging in that mixing ratios drop at the second-highest level but 55 increase slightly at the top height. The interpolation method used in this study allowed for some extrapolation of any CH<sub>4</sub> measured at the top measurement height to ensure more equal weighting of measurements in the flux estimates (see Sect. 2.6 in the main text), suggesting that the interpolation accounted for the majority of this plume's vertical profile. Thus, the CH<sub>4</sub> measured at the top height in this experiment (4.8m) is likely mostly accounted for, and CH<sub>4</sub> would be expected to further 60 decrease at 5.2m in the interpolation. We included this experiment in our dataset and analysis given that the interpolation likely accounted for the majority of CH<sub>4</sub> in this plume and any uncertainties due to missing some CH<sub>4</sub> in the plume's upper tail are likely small relative to uncertainties introduced by atmospheric turbulence.

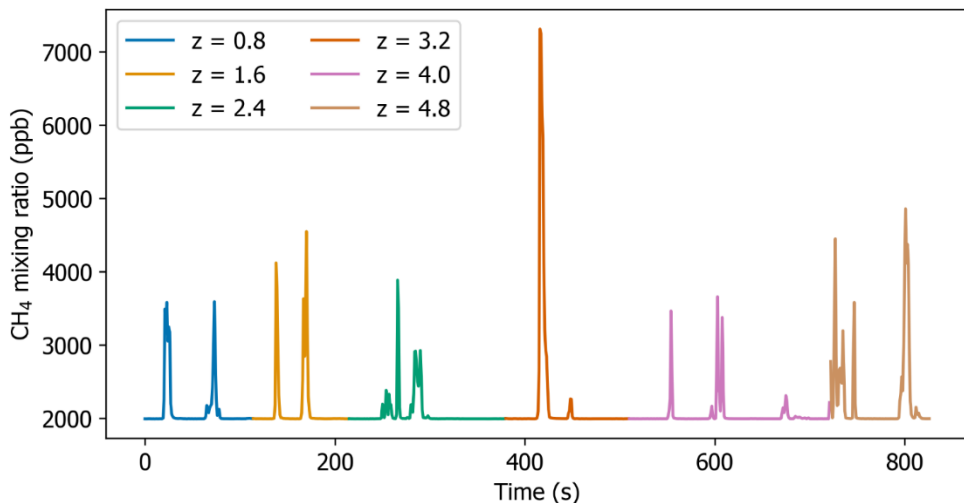


**Fig S1. The 0.41 kg CH<sub>4</sub>/h release performed 30m downwind on 12 June 2024 flagged by our flux plane quality control criterion.**

65 **S6. Data preprocessing steps to horizontally align the CH<sub>4</sub> plume across the walking transects**

We used the SciPy v1.14.1 (Virtanen et al., 2020) “find peaks” package in Python to identify transects from the test measurement heights (we removed the top two measurement heights to test the forward Gaussian method). Identified transects were used in further data processing and emissions quantification with the forward Gaussian method (Fig S2a). It should be noted that two transects were walked for each measurement height, as shown in Fig S2a. The “find peaks” package requires

70 setting height, distance, and prominence parameters. We set the height to the sum of the mean CH<sub>4</sub> mixing ratio across the test  
measurement heights and two standard deviations. In algorithm development and testing, we found this criterion was optimal  
for identifying transects consistent with the key mass of plumes to use in quantifying emissions rates closest to the release  
rates. Distance and prominence parameters were determined by qualitatively examining the time series of measured CH<sub>4</sub>  
75 mixing ratios for the test measurement heights. The goal of setting these parameters was identifying transects that met the  
height criterion for CH<sub>4</sub> based on a single peak value (i.e., the same transect could not be identified twice by the “find peaks”  
package, which could occur in cases where CH<sub>4</sub> was elevated but varied across multiple consecutive measurements if distance  
and prominence parameters were not set optimally).

80

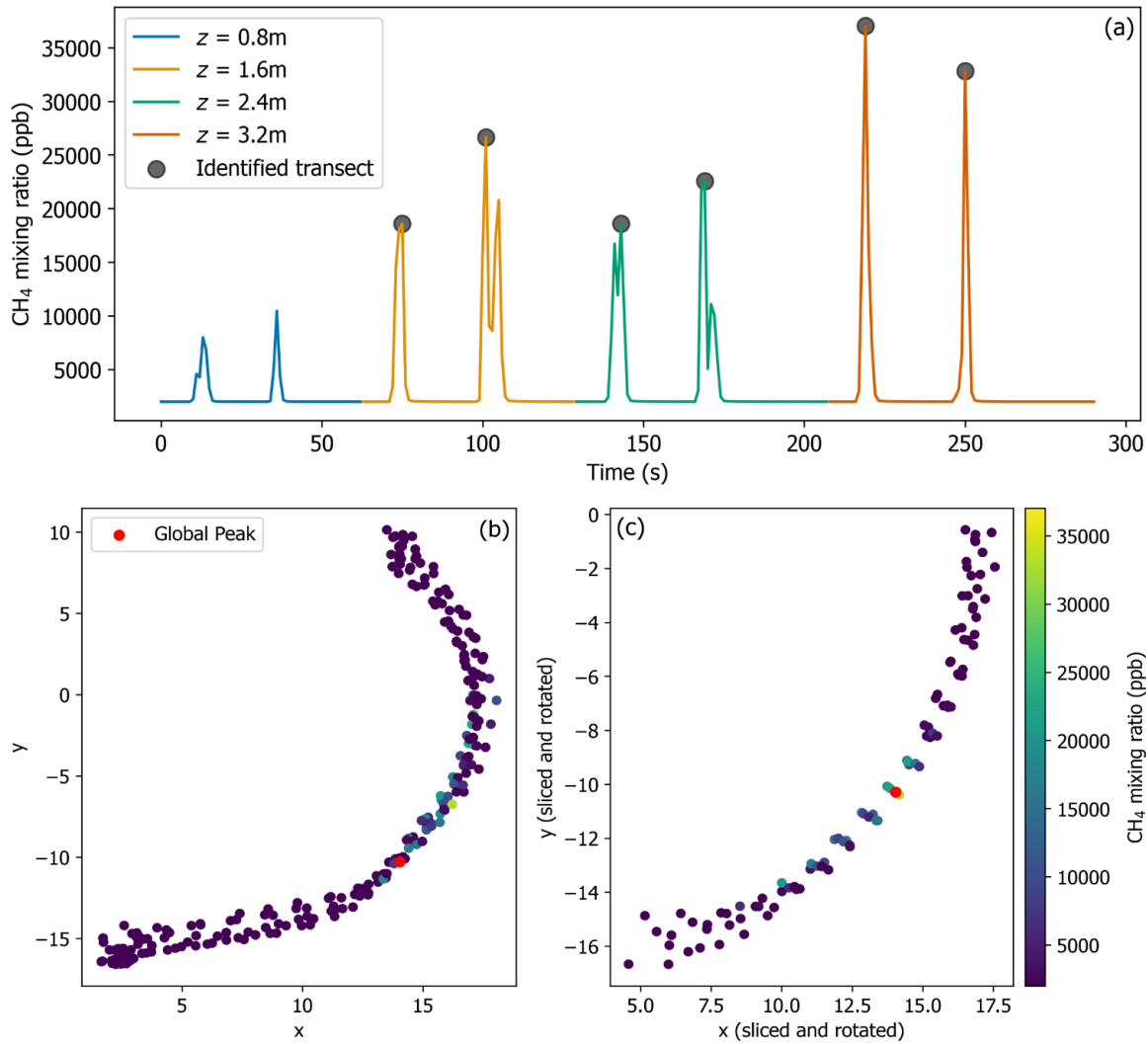
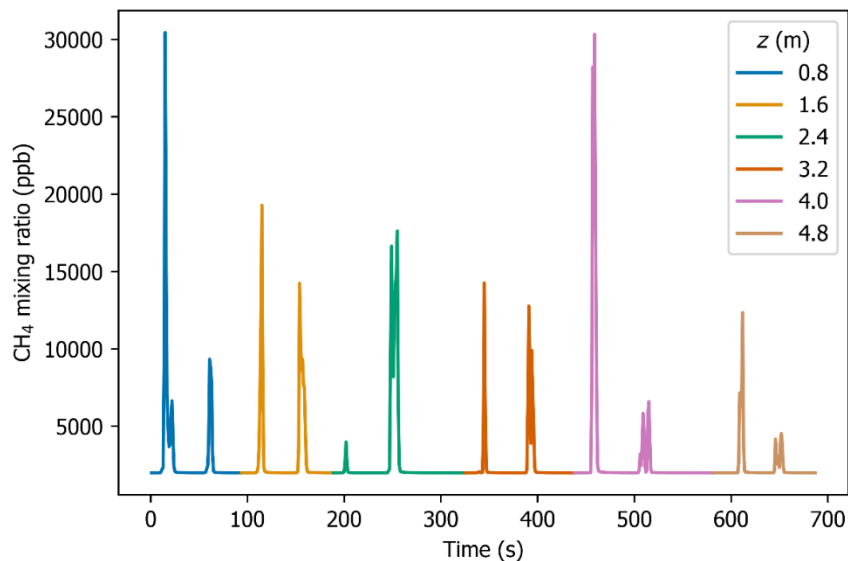


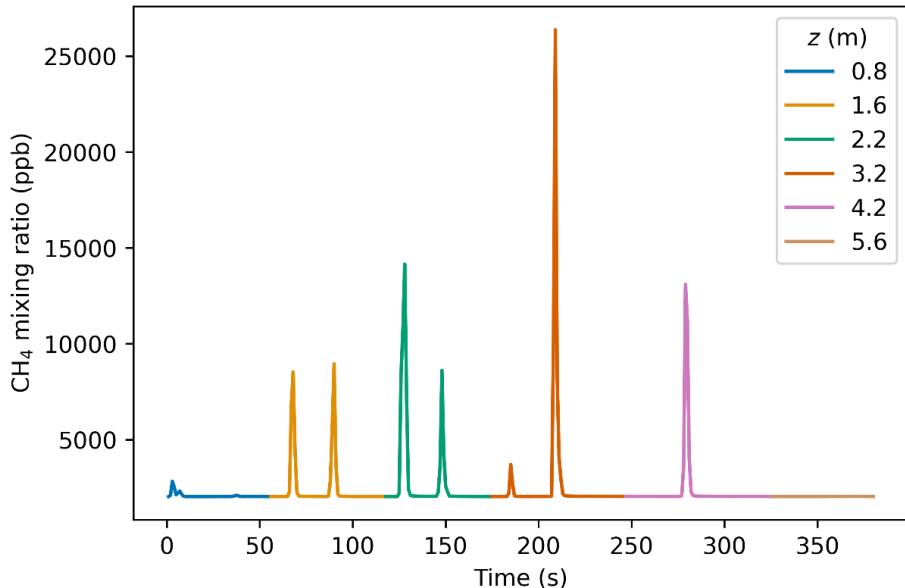
**Fig S2. Data preprocessing of measurements of a 2.4 kg  $\text{CH}_4/\text{h}$  release rate at 15 m downwind distance for the forward Gaussian optimization method (see Sect 2.7 in the main text).** (a) transect identification using SciPy's "find peaks" package in Python by measurement height  $z$  for test measurement heights (see details in the S6 above text). (b) locations of  $\text{CH}_4$  mixing ratios across the identified transects. (c) locations of  $\text{CH}_4$  mixing ratios after data slicing and rotation to horizontally align the plume centerlines from each identified transect. The angle between the global peak shown in (b) and (c)—the measurement with the highest  $\text{CH}_4$  mixing ratio across the test measurement heights—and the release stack (located at 0, 0) was used as the reference wind direction/overall plume centerline to perform the spatial alignment. Data were rotated such that the centerline of each identified transect aligned with the global peak location.

Next, we took slices of CH<sub>4</sub> mixing ratio data from each identified transect centered around the transect peaks shown in Fig S2a. One slice effectively represents when the operator entered, transected, and exited the plume. We determined the data range for the slice by setting an index for seconds elapsed during the experiment and manually confirming that the range captured the operator's pass of the plume within each identified transect. Generally, 5 s to 15 s of data on either side of each peak (Fig S2a) captured the plume passes—including sufficient background data—depending on the downwind distance. We manually confirmed that the data range used for each slice only sliced around the peak of a single transect (i.e., one plume pass).

Finally, we determined the location of the highest CH<sub>4</sub> mixing ratio measured across all test measurement heights (global peak in Fig S2b and S2c). We used the angle between the release stack and this point to represent the reference wind direction/overall plume centerline during the experiments. We rotated the data points from all other identified transects to align the centerlines from those transects with the global peak. Fig S2b shows raw CH<sub>4</sub> mixing ratios from identified transects and Fig S2c shows the sliced, rotated, and aligned data for a 2.4 kg CH<sub>4</sub>/h release rate at 15 m downwind distance on 12 June 2024.



105 **Fig S3. CH<sub>4</sub> mixing ratios measured in the controlled test on 12 June 2024: Release rate 4.8 kg CH<sub>4</sub>/h; downwind distance 30 m.**  
Note the irregular plume shape due to similar mixing ratios measured at 0.8 m and 4.0 m.



110

**Fig S4. CH<sub>4</sub> mixing ratios by height measured in the experiment that produced the largest relative error with the flux plane (141%) and forward Gaussian optimization (223%) methods. The release was 0.31 kg CH<sub>4</sub>/h, and the measurements were performed 10 m downwind on 6 August 2024.**

## References

115 Heier, S.: Grid Integration of Wind Energy: Onshore and Offshore Conversion Systems, 1st ed., Wiley, <https://doi.org/10.1002/9781118703274>, 2014.

Nathan, B. J., Golston, L. M., O'Brien, A. S., Ross, K., Harrison, W. A., Tao, L., Lary, D. J., Johnson, D. R., Covington, A. N., Clark, N. N., and Zondlo, M. A.: Near-Field Characterization of Methane Emission Variability from a Compressor Station Using a Model Aircraft, *Environ. Sci. Technol.*, 49, 7896–7903, <https://doi.org/10.1021/acs.est.5b00705>, 2015.

120 Rella, C. W., Tsai, T. R., Botkin, C. G., Crosson, E. R., and Steele, D.: Measuring Emissions from Oil and Natural Gas Well Pads Using the Mobile Flux Plane Technique, *Environ. Sci. Technol.*, 49, 4742–4748, <https://doi.org/10.1021/acs.est.5b00099>, 2015.

Virtanen, P., Gommers, R., Oliphant, T. E., Haberland, M., Reddy, T., Cournapeau, D., Burovski, E., Peterson, P., Weckesser, W., Bright, J., Van Der Walt, S. J., Brett, M., Wilson, J., Millman, K. J., Mayorov, N., Nelson, A. R. J., Jones, E., Kern, R., 125 Larson, E., Carey, C. J., Polat, İ., Feng, Y., Moore, E. W., VanderPlas, J., Laxalde, D., Perktold, J., Cimrman, R., Henriksen, I., Quintero, E. A., Harris, C. R., Archibald, A. M., Ribeiro, A. H., Pedregosa, F., Van Mulbregt, P., SciPy 1.0 Contributors, Vijaykumar, A., Bardelli, A. P., Rothberg, A., Hilboll, A., Kloeckner, A., Scopatz, A., Lee, A., Rokem, A., Woods, C. N., Fulton, C., Masson, C., Häggström, C., Fitzgerald, C., Nicholson, D. A., Hagen, D. R., Pasechnik, D. V., Olivetti, E., Martin, E., Wieser, E., Silva, F., Lenders, F., Wilhelm, F., Young, G., Price, G. A., Ingold, G.-L., Allen, G. E., Lee, G. R., Audren, H.,

130 Probst, I., Dietrich, J. P., Silterra, J., Webber, J. T., Slavič, J., Nothman, J., Buchner, J., Kulick, J., Schönberger, J. L., De  
Miranda Cardoso, J. V., Reimer, J., Harrington, J., Rodríguez, J. L. C., Nunez-Iglesias, J., Kuczynski, J., Tritz, K., Thoma, M.,  
Newville, M., Kümmeler, M., Bolingbroke, M., Tartre, M., Pak, M., Smith, N. J., Nowaczyk, N., Shebanov, N., Pavlyk, O.,  
Brodtkorb, P. A., Lee, P., McGibbon, R. T., Feldbauer, R., Lewis, S., Tygier, S., Sievert, S., Vigna, S., Peterson, S., More, S.,  
et al.: SciPy 1.0: fundamental algorithms for scientific computing in Python, *Nat Methods*, 17, 261–272,  
135 <https://doi.org/10.1038/s41592-019-0686-2>, 2020.